J Stat Phys (2011) 144:774–792
DOI 10.1007/s10955-011-0256-1

Hydrodynamic Fluctuations in Laminar Fluid Flow. I. Fluctuating Orr-Sommerfeld Equation

J.M. Ortiz de Zárate · J.V. Sengers

Received: 15 March 2011 / Accepted: 16 June 2011 / Published online: 13 July 2011

Abstract In recent years it has become evident that fluctuating hydrodynamics predicts that fluctuations in nonequilibrium states are always spatially long ranged. In this paper we consider the application of fluctuating hydrodynamics to laminar fluid flow, using plane Couette flow as a representative example. Specifically, fluctuating hydrodynamics yields a stochastic Orr-Sommerfeld equation for the wall-normal velocity fluctuations, where spontaneous thermal noise acts as a random source.This stochastic equation needs to be solved subject to appropriate boundary conditions. We show how an exact solution can be obtained from an expansion in terms of the eigenfunctions of the Orr-Sommerfeld hydrodynamic operator. We demonstrate the presence of a flow-induced enhancement of the wall-normal velocity fluctuations and a resulting flow-induced energy amplification and provide a quantitative analysis how these quantities depend on wave number and Reynolds number.

Keywords Hydrodynamic fluctuations · Laminar fluid flow · Plane Couette flow · Orr-Sommerfeld equation

1 Introduction

The theory of fluctuations in fluids that are in thermodynamic equilibrium is well developed on the basis of Landau's fluctuating hydrodynamics [1, 2]. More recently, it has been verified that fluctuating hydrodynamics can be extended to deal with thermally excited fluctuations in fluids in stationary nonequilibrium states. Specifically, fluctuating hydrodynamics has been used to examine in considerable detail temperature and concentration fluctuations in

J.M. Ortiz de Zárate (✉)
Departamento de Física Aplicada I, Facultad de Física, Universidad Complutense, 28040 Madrid, Spain
e-mail: jmortizz@fis.ucm.es

J.V. Sengers
Institute for Physical Science and Technology and Burgers Program for Fluid Dynamics, University of Maryland, College Park, MD 20740-8510, USA
e-mail: sengers@umd.edu

fluids and fluid mixtures subjected to an externally imposed temperature gradient or concentration gradient, as reviewed in a recent monograph [3]. These studies have revealed that the presence of such gradients causes nonequilibrium amplification of the fluctuations that are always long ranged, even far away from any hydrodynamic instability. As a consequence, nonequilibrium fluctuations are generically affected by the presence of boundaries.

The present paper is concerned with the application of fluctuating hydrodynamics to evaluate velocity fluctuations in laminar fluid flow by using plane Couette flow as a representative example. In fluctuating hydrodynamics the usual deterministic hydrodynamic equations are supplemented with random dissipative fluxes of thermal (natural) origin, obeying a fluctuation-dissipation relation. In the case of laminar isothermal flows, one has to consider a random stress tensor representing the stochastic nature of molecular collisions, which are responsible for friction in fluids. Hence, intrinsic "thermal" noise will be always present even for isothermal problems like planar Couette flow. This noise will be amplified by the flow, as is generically expected for any nonequilibrium state [3]. Energy amplification induced by the flow has attracted the interest of many investigators [4–8]. However, in many of these papers the noise is not of thermal origin, does not obey a fluctuation-dissipation relation nor does it have the particular spatial spectrum that is imposed by momentum conservation in molecular collisions. In summary, fluctuating hydrodynamics provides a systematic method for assessing the nature of spontaneous fluctuations in laminar flow induced by intrinsic thermal noise.

The application of fluctuating hydrodynamics to shear flows has been initiated by a number of investigators, but without consideration of any confinement effects [9–13]. However, the long-ranged spatial nature of the fluctuations is highly anisotropic and for certain directions of the wave vector the fluctuations will encompass the entire fluid system, so that boundary effects need to be accounted for. For this reason we have initiated a research project aimed at a detailed evaluation of the intensity of velocity fluctuations of thermal origin in plane Couette flow [14–16]. We started by linearizing the hydrodynamic equations for the fluctuations and derived fluctuating Orr-Sommerfeld and Squire equations to describe wall-normal velocity and vorticity fluctuations, respectively. These equations are the stochastic versions of the deterministic Orr-Sommerfeld and Squire equations traditionally discussed in the linear stability analysis of laminar flows [17, 18]. It is well known that, for laminar plane Couette flow or laminar pipe flow, a traditional linear instability analysis, based on infinitesimal perturbations, does not yield a critical value of the Reynolds number associated with a transition from laminar to turbulent flow, and these flows are always linearly stable [17–21]. For similar reasons, linearized fluctuating hydrodynamics cannot explain the nature of the instability, but it will be relevant at moderate Reynolds numbers, as long as the laminar state is clearly stable. Furthermore, since the intensity of the thermal fluctuations depends strongly on the wave vector, fluctuating hydrodynamics may identify the least stable modes, a knowledge that could be helpful in developing possible nonlinear models.

Our previous solutions of the stochastic Orr-Sommerfeld and Squire equations were based on semi-quantitative Galerkin approximations to accommodate realistic boundary conditions. We have subsequently obtained exact solutions of these stochastic equations in the presence of boundaries by formulating an expansion of the eigenfunctions (normal modes) of the hydrodynamic operator. These exact solutions enable us to test the quality of the Galerkin approximations. The purpose of the present paper is to present such an analysis for the stochastic Orr-Sommerfeld equation. Our main aim is to analyze the wave-vector dependence (spatial spectrum) of the intensity of the intrinsic thermal velocity fluctuations at moderate Reynolds numbers. The solution of the stochastic Squire equation will be presented in a subsequent publication.

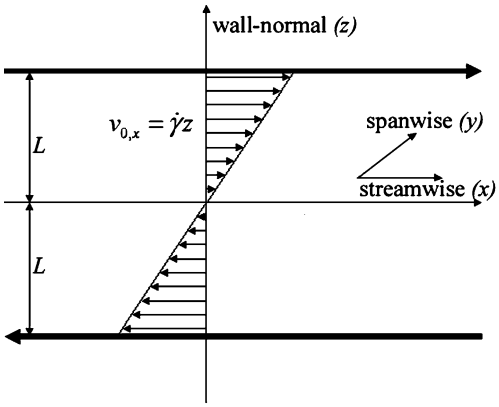

Fig. 1 Schematic representation of plane Couette flow

We shall proceed as follows. In Sect. 2 we recall the form of the stochastic Orr-Sommerfeld equation for the wall-normal velocity fluctuations. In Sect. 3 we sketch the procedure for solving the stochastic Orr-Sommerfeld equation and we derive an expression for the autocorrelation function of the wall-normal velocity fluctuations. Section 4 contains the main results of this paper, where we discuss the intensity of the intrinsic flow-induced wall-normal velocity fluctuations, as a function of the wave number and the Reynolds number, and make a comparison with our previous Galerkin-based estimates. We conclude with a discussion of the results in Sect. 5. Some technical aspects of the analysis are presented in an Appendix.

2 Stochastic Orr-Sommerfeld Equation

We consider a liquid with uniform temperature T under incompressible laminar flow (thus with uniform density ρ) between two horizontal boundaries separated by a distance $2L$, as indicated schematically in Fig. 1. We adopt a coordinate system with the X axis in the streamwise direction, the Y axis in the spanwise direction, and the Z axis in the wall-normal direction. This coordinate system agrees with the one adopted by Drazin and Reid [18] and has been referred to as the meteorological convention [8]. The stationary velocity $\mathbf{v}_0 = \{\dot{\gamma} z, 0, 0\}$ is in the X direction and depends linearly on the vertical coordinate with a constant shear rate $\dot{\gamma}$. It is convenient to use a dimensionless position variable $\mathbf{r}$ measured in terms of the length L, a dimensionless time t obtained by multiplying the actual time with the shear rate $\dot{\gamma}$, a dimensionless fluid velocity $\mathbf{v}$ in terms of the product $L\dot{\gamma}$, and a dimensionless stress tensor Π in terms of $\rho L^2 \dot{\gamma}$. As shown in a previous publication [14], fluctuating hydrodynamics then yields for the fluctuations of the wall-normal component δv_z of the fluctuating dimensionless velocity $\delta\mathbf{v}$ a stochastic Orr-Sommerfeld equation of the form:

$$\partial_t(\nabla^2 \delta v_z) + z\partial_x(\nabla^2 \delta v_z) - \frac{1}{\mathrm{Re}}\nabla^4(\delta v_z) = \left\{\nabla \times \nabla \times \left[\nabla(\delta\Pi)\right]\right\}_z, \tag{1}$$

where Re is the Reynolds number

$$\mathrm{Re} = \frac{\dot{\gamma} L^2}{\nu} \tag{2}$$

with ν being the kinematic viscosity of the fluid. One recognizes in (1) the usual Orr-Sommerfeld equation for plane Couette flow, but with an extra stochastic forcing term, expressed as derivatives of a random stress tensor $\delta\Pi(\mathbf{r}, t)$. In accordance with the guidelines of fluctuating hydrodynamics [1, 3], Newton's viscosity law is modified by the addition of a stochastic contribution $\delta\Pi(\mathbf{r}, t)$ to the stress tensor that accounts for the random nature of molecular collisions. Then, substitution of the new expression for the stress tensor into the momentum-balance equation yields a stochastic Navier-Stokes equation. Since the random contribution to the stress tensor averages to zero over the fluctuations, $\langle\delta\Pi(\mathbf{r}, t)\rangle = 0$, the mean stationary solution of the stochastic Navier-Stokes equation, $\mathbf{v}_0(\mathbf{r})$, is the same as if thermal fluctuations were not present. However, because of the noise term, there will be spontaneous thermal velocity fluctuations around the steady-state solution. Equation (1) is then obtained by substituting $\mathbf{v}_0(\mathbf{r}) + \delta\mathbf{v}(\mathbf{r}, t)$ for the velocity into the stochastic Navier-Stokes equation and taking a double curl [14].

The presence of the random noise term makes (1) a Langevin-like stochastic partial differential equation, $\delta v_z(\mathbf{r}, t)$ being now a dependent stochastic field and $\delta\Pi(\mathbf{r}, t)$ an independent stochastic forcing. Our goal is to obtain the statistical properties (autocorrelation function) of $\delta v_z(\mathbf{r}, t)$ from the known statistical properties of the thermal noise $\delta\Pi(\mathbf{r}, t)$. The latter are given by the fluctuation-dissipation theorem, that for an incompressible fluid reads [1, 3, 22, 23]:

$$\left\langle \delta\Pi_{ij}(\mathbf{r}, t) \cdot \delta\Pi_{kl}(\mathbf{r}', t') \right\rangle = 2\tilde{S}(\delta_{ik}\delta_{jl} + \delta_{il}\delta_{jk})\delta(\mathbf{r} - \mathbf{r}')\delta(t - t'), \tag{3}$$

where $\tilde{S}$ is the dimensionless strength of the thermal noise [14]:

$$\tilde{S} = \frac{k_B T}{\dot{\gamma}^3 L^7}\frac{\nu}{\rho} = \frac{k_B T}{\rho L^3}\frac{1}{\dot{\gamma}^2 L^2}\frac{1}{\mathrm{Re}}, \tag{4}$$

with k_B being the Boltzmann constant. The correlation functions of random dissipative fluxes, as given by (3) for $\delta\Pi(\mathbf{r}, t)$, are short ranged in time (Markov processes) as well as in space. In the hydrodynamic limit this short-ranged nature is represented by delta functions, as in the right-hand side (RHS) of (3). The fluctuation-dissipation theorem (3) is to be expressed in terms of the local values of the appropriate thermodynamic and transport properties. The validity of adopting such a local version of the fluctuation-dissipation theorem for dealing with thermal fluctuations in nonequilibrium states has now been well established [3, 22–24].

We emphasize that balance of momentum causes the presence of a double curl and a divergence acting upon the random stress tensor in (1). This gives the stochastic forcing a characteristic spatial spectrum that will influence the spatial spectrum of the velocity fluctuations. Finally, we note that the actual correlation function of the fluctuating stress tensor only depends on the properties of the fluid (namely, temperature and kinematic viscosity); the Reynolds number appears in (4) only as a consequence of the manner in which the stress tensor has been made dimensionless.

Equation (1) needs to be solved for the wall-normal velocity fluctuation $\delta v_z(\mathbf{r}, t)$ subject to realistic boundary conditions:

$$\delta v_z = \partial_z \delta v_z = 0, \quad \text{at } z = \pm 1. \tag{5}$$

Equations (1)–(5) determine the intrinsic wall-normal velocity fluctuations and the resulting energy amplification, as will be shown in this paper.

3 Procedure for Solving the Orr-Sommerfeld Equation

To solve (1) with the boundary conditions (5) at $z = \pm 1$, we apply a Fourier transform in time and in the horizontal xy-plane. The resulting expression can be written as:

$$[\mathrm{i}\omega\mathcal{D} + \mathcal{H}] \cdot \delta v_z(\omega, \mathbf{q}_\parallel, z) = F(\omega, \mathbf{q}_\parallel, z), \tag{6}$$

where we have introduced two (linear) differential operators:

$$\mathcal{H} = \mathrm{i}zq_x\left(\partial_z^2 - q_\parallel^2\right) - \frac{1}{\mathrm{Re}}\left(\partial_z^2 - q_\parallel^2\right)^2, \tag{7}$$

and

$$\mathcal{D} = \left(\partial_z^2 - q_\parallel^2\right). \tag{8}$$

The differential operator $\mathcal{H}$ is commonly referred to as the hydrodynamic operator. In (6)–(8), $\mathbf{q}_\parallel = \{q_x, q_y\}$ represents the wave vector of the fluctuations in the horizontal plane and $q_\parallel^2 = q_x^2 + q_y^2$. Furthermore, in (6), $F(\omega, \mathbf{q}_\parallel, z)$ represents an additive random noise term given by the Fourier transformation in time and in the horizontal plane of the RHS of (1). Equation (6) has to be solved subject to the boundary conditions (5), or equivalently:

$$\delta v_z(\omega, \mathbf{q}_\parallel, z) = \partial_z \delta v_z(\omega, \mathbf{q}_\parallel, z) = 0, \quad \text{at } z = \pm 1. \tag{9}$$

It is possible to find such a solution by expanding the hydrodynamic operator in a series of normal modes. For completeness we sketch here briefly the procedure and refer the interested reader to the relevant literature [17, 18] for details. Specifically, we consider the following eigenvalue problem:

$$\mathcal{H} \cdot R_N(\mathbf{q}_\parallel, z) = \Gamma_N(\mathbf{q}_\parallel)\left[\mathcal{D} \cdot R_N(\mathbf{q}_\parallel, z)\right], \tag{10}$$

where $\Gamma_N(\mathbf{q}_\parallel)$ are the eigenvalues (decay rates), and where the right eigenfunctions $R_N(\mathbf{q}_\parallel, z)$ have to satisfy the boundary conditions

$$R_N(\mathbf{q}_\parallel, z) = \partial_z R_N(\mathbf{q}_\parallel, z) = 0, \quad \text{at } z = \pm 1. \tag{11}$$

It can be demonstrated [17, 18] that, for given $\mathbf{q}_\parallel$, there exists an infinite numerable set of solutions to (10), and the index N distinguishes among them (see Appendix). To complete the formulation of the eigenvalue problem we need also to consider the adjoint operator [17, 18]:

$$\mathcal{H}^\dagger = -\mathrm{i}zq_x\left(\partial_z^2 - q_\parallel^2\right) - \frac{1}{\mathrm{Re}}\left(\partial_z^2 - q_\parallel^2\right)^2 - 2\mathrm{i}q_x\partial_z, \tag{12}$$

and left eigenfunctions $L_N(\mathbf{q}_\parallel, z)$ such that:

$$\mathcal{H}^\dagger \cdot L_N(\mathbf{q}_\parallel, z) = \Gamma_N^*(\mathbf{q}_\parallel)\left[\mathcal{D} \cdot L_N(\mathbf{q}_\parallel, z)\right], \tag{13}$$

where the left eigenfunctions $L_N(\mathbf{q}_\parallel, z)$ should satisfy the same boundary conditions (11) as the right ones. In (13) we anticipated that the eigenvalues of the adjoint operator are

the complex conjugate (Γ_N^*) of the eigenvalues of $\mathcal{H}$ (see Appendix). The set of right/left eigenfunctions form a biorthogonal set [18], in the sense that:

$$\int_{-1}^{1} L_M^*(\mathbf{q}_\parallel, z)\big[\mathcal{D} \cdot R_N(\mathbf{q}_\parallel, z)\big]\, dz = B_N(\mathbf{q}_\parallel)\delta_{NM}, \tag{14}$$

where $B_N(\mathbf{q}_\parallel)$ has to be interpreted as the "norm" of the eigenpair $\{R_N(\mathbf{q}_\parallel, z), L_N(\mathbf{q}_\parallel, z)\}$:

$$\begin{aligned} B_N(\mathbf{q}_\parallel) &= \int_{-1}^{1} L_N^*(\mathbf{q}_\parallel, z)\big[\mathcal{D} R_N(\mathbf{q}_\parallel, z)\big]\, dz \\ &= \int_{-1}^{1} \big[\mathcal{D} L_N^*(\mathbf{q}_\parallel, z)\big] R_N(\mathbf{q}_\parallel, z)\, dz. \end{aligned} \tag{15}$$

We are now ready to solve our original problem, (6), by expanding the solution in a series of (right) eigenfunctions:

$$\delta v_z(\omega, \mathbf{q}_\parallel, z) = \sum_{N=0}^{\infty} G_N^{\mathrm{R}}(\omega, \mathbf{q}_\parallel) R_N(\mathbf{q}_\parallel, z). \tag{16}$$

If we substitute (16) into (6), make use of (10), and project the result over an arbitrary left eigenfunction $L_M(\mathbf{q}_\parallel, z)$, we obtain, with the biorthogonality condition (14), an expression for the coefficients in the series expansion (16), namely:

$$G_N^{\mathrm{R}}(\omega, \mathbf{q}_\parallel) = \frac{F_N(\omega, \mathbf{q}_\parallel)}{B_N(\mathbf{q}_\parallel)[\mathrm{i}\omega + \Gamma_N(\mathbf{q}_\parallel)]} \tag{17}$$

with $F_N(\omega, \mathbf{q}_\parallel)$ being the projections of the random noise onto the left eigenfunctions:

$$F_N(\omega, \mathbf{q}_\parallel) = \int_{-1}^{1} L_N^*(\mathbf{q}_\parallel, z) \cdot F(\omega, \mathbf{q}_\parallel, z)\, dz. \tag{18}$$

Equation (18) also indicates the general way of projecting an arbitrary function $F(z)$ over a left eigenfunction.

The main difference with an evaluation procedure of the corresponding deterministic equation [17, 18] is that we shall also need here the statistical correlations among the various projections $F_N(\omega, \mathbf{q}_\parallel)$ of the random noise. For the same random noise term $F(\omega, \mathbf{q}_\parallel, z)$ in (6), these correlations have been considered in a recent monograph [3], but with a different set of eigenfunctions. Upon following the same procedure [3], it is relatively simple to see that these correlation functions can be expressed as:

$$\big\langle F_N^*(\omega, \mathbf{q}_\parallel) \cdot F_M(\omega', \mathbf{q}_\parallel')\big\rangle = \tilde{S}\, \Xi_{NM}(\mathbf{q}_\parallel)(2\pi)^3 \delta(\omega - \omega')\delta(\mathbf{q}_\parallel - \mathbf{q}_\parallel'), \tag{19}$$

where, following Schmitz and Cohen [22, 23], we have introduced mode-coupling coefficients:

$$\Xi_{NM}(\mathbf{q}_\parallel) = 2q_\parallel^2 \int_{-1}^{1} dz \big[\mathcal{D}^2 L_N(\mathbf{q}_\parallel, z)\big] L_M^*(\mathbf{q}_\parallel, z). \tag{20}$$

Using the adjoint problem (13) and the boundary conditions (11), we can further simplify expression (20) for $\Xi_{NM}(\mathbf{q}_\parallel)$ to obtain

$$\Xi_{NM}(\mathbf{q}_\parallel) = -q_\parallel^2 \,\mathrm{Re}\big\{\big[\Gamma_N^*(\mathbf{q}_\parallel) + \Gamma_M(\mathbf{q}_\parallel)\big]\Xi_{NM}^{(\mathrm{E})}(\mathbf{q}_\parallel) + q_x \,\mathrm{Re}^2\, \Xi_{NM}^{(\mathrm{NE})}(\mathbf{q}_\parallel)\big\}, \tag{21}$$

where we have separated the mode-coupling coefficients into two parts:

$$\Xi^{(\mathrm{E})}_{NM}(\mathbf{q}_\parallel) = \int_{-1}^{1} dz \big[\mathcal{D}L_N(\mathbf{q}_\parallel, z)\big] L^*_M(\mathbf{q}_\parallel, z), \tag{22}$$

$$\Xi^{(\mathrm{NE})}_{NM}(\mathbf{q}_\parallel) = \frac{2\mathrm{i}}{\mathrm{Re}^2} \int_{-1}^{1} dz \big[\partial_z L_N(\mathbf{q}_\parallel, z)\big] L^*_M(\mathbf{q}_\parallel, z). \tag{23}$$

The decomposition (21) of the mode-coupling coefficients will enable us to separate the equal-time autocorrelation function of the wall-normal velocity fluctuations into an equilibrium and a nonequilibrium part. In the definition (21) of the nonequilibrium mode-coupling coefficient $\Xi^{(\mathrm{NE})}_{NM}$, we have extracted a factor $q_x\,\mathrm{Re}^2$ to emphasize the Squire symmetry of the problem, to be discussed later.

From the preceding analysis, combining (16) and (19) and averaging over fluctuations, we conclude that the autocorrelation function of wall-normal velocity fluctuations can be expressed as:

$$\big\langle \delta v_z^*(\omega, \mathbf{q}_\parallel, z) \cdot \delta v_z(\omega', \mathbf{q}'_\parallel, z') \big\rangle = C_{zz}(\omega, \mathbf{q}_\parallel, z, z')(2\pi)^3 \delta(\omega - \omega')\delta(\mathbf{q}_\parallel - \mathbf{q}'_\parallel), \tag{24}$$

where $C_{zz}(\omega, \mathbf{q}_\parallel, z, z')$ is a double series of right eigenfunctions. Here we are interested in the equal-time correlation function which determines the intensity of the fluctuations. After applying inverse Fourier transforms in ω and ω' to (24), we can express the equal-time correlation function as:

$$\big\langle \delta v_z^*(\mathbf{q}_\parallel, z, t) \cdot \delta v_z(\mathbf{q}'_\parallel, z', t) \big\rangle = C_{zz}(\mathbf{q}_\parallel, z, z')(2\pi)^2 \delta(\mathbf{q}_\parallel - \mathbf{q}'_\parallel) \tag{25}$$

with the static correlation function

$$C_{zz}(\mathbf{q}_\parallel, z, z') = \frac{1}{2\pi} \int_{-\infty}^{\infty} C_{zz}(\omega, \mathbf{q}_\parallel, z, z')\, d\omega. \tag{26}$$

Next, we combine (16) and (17), and use (19) to obtain $C_{zz}(\omega, q_\parallel, z, z')$ in (24). If we then substitute this result into (26) the integral over the frequency can be performed, since all the decay rates Γ_N have a non-zero real part [25, 26]. We then obtain an explicit expression for the equal-time (static) autocorrelation function in terms of the hydrodynamic modes:

$$C_{zz}(z, z') = \tilde{S} \sum_{N,M=0}^{\infty} \frac{\Xi_{NM} R^*_N(z) R_M(z')}{B^*_N B_M [\Gamma^*_N + \Gamma_M]}, \tag{27}$$

where for ease of notation we did not indicate explicitly the dependence on the wave vector $\mathbf{q}_\parallel$. With the help of the decomposition (21) of the mode-coupling coefficients, we also separate the equal-time autocorrelation function $C_{zz}(\mathbf{q}_\parallel, z, z')$ into an equilibrium and a nonequilibrium part:

$$C_{zz}(\mathbf{q}_\parallel, z, z') = C^{(\mathrm{E})}_{zz}(\mathbf{q}_\parallel, z, z') + C^{(\mathrm{NE})}_{zz}(\mathbf{q}_\parallel, z, z'), \tag{28}$$

with

$$\frac{C^{(\mathrm{E})}_{zz}(z, z')}{\tilde{S}\,\mathrm{Re}} = -q_\parallel^2 \sum_{N,M=0}^{\infty} \frac{\Xi^{(\mathrm{E})}_{NM} R^*_N(z) R_M(z')}{B^*_N B_M}, \tag{29}$$

$$\frac{C^{(\mathrm{NE})}_{zz}(z, z')}{\tilde{S}\,\mathrm{Re}} = -q_\parallel^2 \sum_{N,M=0}^{\infty} \frac{q_x\,\mathrm{Re}^2\, \Xi^{(\mathrm{NE})}_{NM} R^*_N(z) R_M(z')}{B^*_N B_M [\Gamma^*_N + \Gamma_M]}. \tag{30}$$

To simplify (29), we can use the fact that:

$$\delta(\xi - z') = \sum_{N=0}^{\infty} \frac{(\partial_\xi^2 - q_\parallel^2) L_N^*(\mathbf{q}_\parallel, \xi)}{B_N(\mathbf{q}_\parallel)} R_N(\mathbf{q}_\parallel, z'), \tag{31}$$

which is obtained by expanding $\delta(\xi - z')$ in a series of right eigenfunctions, which, as a function of z', fulfill the relevant boundary conditions. Then, combining (31) and the explicit expression (22) for $\Xi_{NM}^{(\mathrm{E})}(\mathbf{q}_\parallel)$, the sum over one of the indices in (29) can be performed exactly, and the correlation function $C_{zz}^{(\mathrm{E})}(\mathbf{q}_\parallel, z, z')$ becomes:

$$C_{zz}^{(\mathrm{E})}(z, z') = -\tilde{S}\,\mathrm{Re}\, q_\parallel^2 \sum_{N=0}^{\infty} \frac{R_N^*(z)}{B_N^*} L_N(z'). \tag{32}$$

Equation (32) can be further simplified by applying the differential operator $(\partial_{z'}^2 - q_\parallel^2)$ to $C_{zz}^{(\mathrm{E})}(\mathbf{q}_\parallel, z, z')$, so that, in view of (31), the resulting expression becomes proportional to a delta function $\delta(z - z')$. We thus obtain a differential equation for $C_{zz}^{(\mathrm{E})}(\mathbf{q}_\parallel, z, z')$ that can be easily integrated by using the fact that, for any z', $C_{zz}^{(\mathrm{E})}(\mathbf{q}_\parallel, z, z')$ vanishes at both $z = +1$ and $z = -1$. Following this procedure we can sum the series (32) and obtain:

$$C_{zz}^{(\mathrm{E})}(\mathbf{q}_\parallel, z, z') = \tilde{S}\,\mathrm{Re}\,\frac{q_\parallel}{2}\left[\frac{\cosh(q_\parallel|z - z'|)}{\tanh 2q_\parallel} - \frac{\cosh(q_\parallel|z + z'|)}{\sinh 2q_\parallel} - \sinh(q_\parallel|z - z'|)\right], \tag{33}$$

which, when reverted to units with physical dimensions, is independent of the shear rate $\dot{\gamma}$ and, hence, represents a true equilibrium contribution. We have also verified (33) by numerically evaluating up to eight of the lower hydrodynamic modes $R_N(\mathbf{q}_\parallel, z)$ for $\mathrm{Re} = 0$ (see Appendix), substituting the results into (29), and observing a fast (numerical) convergence to (33).

Further confirmation of (33) can be obtained by noticing that in the "bulk" $q_\parallel \to \infty$ limit one can adopt the approximations $\tanh 2q_\parallel \simeq 1$ and $\sinh 2q_\parallel \simeq \infty$. Then

$$C_{zz}^{(\mathrm{E})}(\mathbf{q}_\parallel, z, z') \overset{q_\parallel \to \infty}{\longrightarrow} \tilde{S}\,\mathrm{Re}\,\frac{q_\parallel}{2}\exp(-q_\parallel|z - z'|). \tag{34}$$

From which, upon substitution into (25) and application of a double Fourier transformation in z and z', we obtain:

$$\left\langle \delta v_z^*(\mathbf{q}, t) \cdot \delta v_z(\mathbf{q}', t) \right\rangle^{(\mathrm{E})} \overset{q_\parallel \to \infty}{\longrightarrow} \frac{\tilde{S}\,\mathrm{Re}\, q_\parallel^2}{q_\parallel^2 + q_z^2} (2\pi)^3 \delta(\mathbf{q} - \mathbf{q}'), \tag{35}$$

which reproduces the well-known result for the intensity of transverse-velocity fluctuations from the theory of fluctuations in bulk equilibrium fluids (*i.e.*, without accounting for boundary conditions) [27, 28].

In summary, the main result of this section is (28), which shows that the intensity of velocity fluctuations is the sum of an equilibrium contribution, given by (33) for $C_{zz}^{(\mathrm{E})}(\mathbf{q}_\parallel, z, z')$, and a nonequilibrium contribution given by (30). This structure appears to be a universal feature of fluids in nonequilibrium states [3, 29], for which mode-coupling phenomena generically enhance the intensity of thermal fluctuations. The existence of such enhancements has been demonstrated experimentally for fluids in the presence of temperature gradients [3].

4 Nonequilibrium Enhancement of the Wall-Normal Velocity Fluctuations

The nonequilibrium enhancement of spontaneous velocity fluctuations induced by the flow is given by $C_{zz}^{(\mathrm{NE})}(\mathbf{q}_\parallel, z, z')$ in (30) in terms of the hydrodynamic normal modes and their corresponding decay rates. These modes have been discussed extensively in the literature [17, 18], and we could build on these results to evaluate the intensity $C_{zz}^{(\mathrm{NE})}(\mathbf{q}_\parallel, z, z')$ numerically. However, we are primarily interested in the wave-vector dependence of the nonequilibrium enhancement of the intensity of the fluctuations and, hence, in the wavenumber dependence of the decay rates. Since a comprehensive analysis of the wave-vector dependence is not common, we have performed our own (medium resolution) numerical computation of the decay rates. For this purpose we find it advantageous to use the explicit expressions of the normal modes in terms of Airy functions due to Romanov [25] and Dyachenko and Shkalikov [26]. For completeness, we present the expressions in the Appendix, while we here discuss only how they can be used to evaluate the decay rates and the nonequilibrium wall-normal velocity correlation function numerically.

4.1 Numerical Computation of Decay Rates

We prefer to write the decay rates $\Gamma_N(\mathbf{q}_\parallel)$ in (30) as

$$\Gamma_N(\mathbf{q}_\parallel) = q_x a_N(\mathbf{q}_\parallel) + \frac{q_\parallel^2}{\mathrm{Re}}. \tag{36}$$

In the Appendix we show how $a_N(\mathbf{q}_\parallel)$ and, hence, the decay rates $\Gamma_N(\mathbf{q}_\parallel)$, can be determined by expressing the eigenfunctions of the hydrodynamic operator in terms of Airy functions. We have obtained $a_N(\mathbf{q}_\parallel)$ as a function of $q_\parallel$ for several values of the effective Reynolds number $\overline{\mathrm{Re}} = \mathrm{Re}\cos\varphi$ (with φ being the azimuthal angle of $\mathbf{q}_\parallel$) by solving (51) in the Appendix numerically using commercial software. Rather than converting these results into the actual decay rates through (36), we shall present instead the results obtained directly for $a_N(\mathbf{q}_\parallel)$ to which we, for convenience, also refer as "decay rates" in this subsection. Since we are interested in the decay rates as a function of the wave number $q_\parallel$ of the fluctuations, our plots differ slightly from those commonly shown in the literature [17, 18, 30]. We first display in Fig. 2 the eight lowest "decay rates", $a_0(q_\parallel)$ through $a_7(q_\parallel)$, as a function of $q_\parallel$ for an effective Reynolds number $\overline{\mathrm{Re}} = 25$. The upper panel shows the real part and the lower panel the imaginary part of a_N.

As can be seen from Fig. 2, the decay rates are real numbers at low values of $q_\parallel$. However, after a certain non-zero value of $q_\parallel$, the real parts of pairs of decay rates merge and the two merged decay rates become pairs of complex conjugate numbers. When two decay rates converge to form a complex conjugate pair, it means that the modes become *propagating*, because the thermally excited velocity perturbations have time to oscillate before decaying to zero. At large enough values of $q_\parallel$ only such propagating modes are present.

Other consequences that can be inferred from Fig. 2 are: for $q_\parallel \to 0$ the $a_N(q_\parallel)$ become proportional to $q_\parallel^{-1}$; for $q_\parallel \to \infty$ the real parts of the complex conjugate pairs of $a_N(q_\parallel)$ decay to zero proportionally to $q_\parallel^{-1/3}$, while the imaginary parts exponentially approach $\pm\mathrm{i}$. These asymptotic dependencies of the decay rates on $q_\parallel$ can also be derived analytically by solving (50) perturbatively [25, 30].

Another interesting feature is a qualitative difference in the dependence of the decay rates $a_N(q_\parallel)$ on $q_\parallel$ at small and larger values of $\overline{\mathrm{Re}}$. To illustrate this difference, we show in Fig. 3 plots of the real parts of the four lower a_N as a function of $q_\parallel$ for $\overline{\mathrm{Re}} = 25$ (left panel)

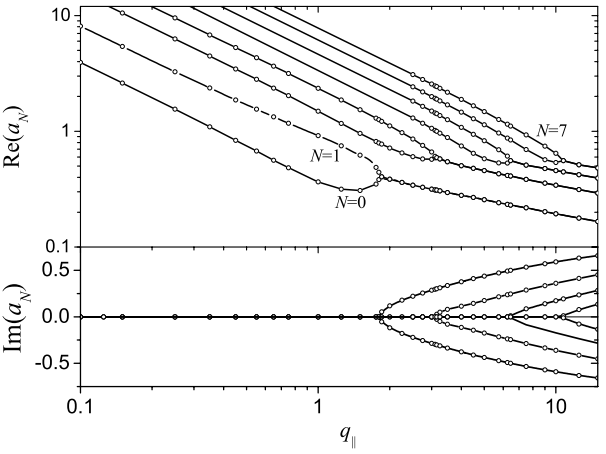

Fig. 2 Real (*upper panel*) and imaginary (*lower panel*) parts of the eight slowest decay rates as a function of $q_\parallel$, for an effective Reynolds number $\overline{\mathrm{Re}} = 25$

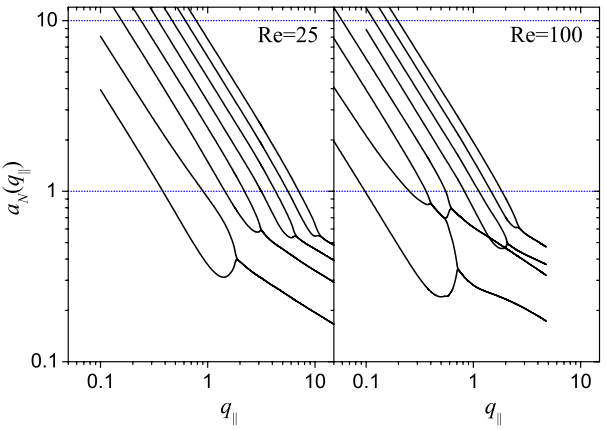

Fig. 3 Real part of the eight lower decay rates for effective Reynolds numbers $\overline{\mathrm{Re}} = 25$ and $\overline{\mathrm{Re}} = 100$. Notice the different qualitative behavior, since at larger $\overline{\mathrm{Re}}$ there exists a window of wave numbers where the second and the third decay rates form a complex conjugate pair

and for $\overline{\mathrm{Re}} = 100$ (right panel). At the larger value of $\overline{\mathrm{Re}}$ (right panel) we find a crossover between the second and third decay rate at intermediate values of $q_\parallel$ which is absent at the lower value of $\overline{\mathrm{Re}}$ (left panel). It turns out that the transition from the behavior shown in the left panel to that shown in the right panel occurs at $\overline{\mathrm{Re}} \simeq 63$. At larger values of $\overline{\mathrm{Re}}$ the landscape indicating the dependence of the various decay rates on $q_\parallel$ becomes progressively more complicated with multiple crossovers appearing between different pairs of $a_N(q_\parallel)$.

To conclude the discussion of the decay rates we emphasize, as demonstrated by Romanov [25, 30], that the real parts of the decay rates do not exhibit a change of sign at any value of the Reynolds number. Hence, integrations leading to (30) are justified and we do not find fluctuations with a diverging intensity due to a vanishing value of the real part of a decay rate. This observation agrees with the well-known fact that a linear theory by itself does not account for the appearance of instability in planar Couette flow [17, 18, 20].

4.2 Numerical Computation of the Wall-Normal Velocity Correlation Function

From (25) we see that the correlation function $\langle \delta v_z^*(\mathbf{q}_\parallel, z, t) \cdot \delta v_z(\mathbf{q}'_\parallel, z', t) \rangle$ is translationally invariant in the horizontal plane (parallel to the walls), but, as a consequence of the boundary conditions, it is not translationally invariant in the z-direction. As we have discussed

elsewhere [14, 15], this problem can be dealt with by integrating the correlation function $C_{zz}(\mathbf{q}_\parallel, z, z')$ in (25) over the height of the fluid layer to obtain a two-point mean correlation function as a function of the wave vector in the horizontal plane:

$$C_{zz}(\mathbf{q}_\parallel) = \frac{1}{2}\int_{-1}^{1} dz \int_{-1}^{1} dz'\, C_{zz}(\mathbf{q}_\parallel, z, z'). \tag{37}$$

As a consequence of (28), the averaged correlation function (or spatial spectrum of the fluctuations) $C_{zz}(\mathbf{q}_\parallel)$ is also the sum of two contributions: $C_{zz}(\mathbf{q}_\parallel) = C_{zz}^{(\mathrm{E})}(\mathbf{q}_\parallel) + C_{zz}^{(\mathrm{NE})}(\mathbf{q}_\parallel)$. The equilibrium contribution $C_{zz}^{(\mathrm{E})}(\mathbf{q}_\parallel)$ is obtained by substituting (33) into (37). Some simple integrations yield:

$$C_{zz}^{(\mathrm{E})}(\mathbf{q}_\parallel) = \tilde{S}\,\mathrm{Re}\left[1 + \frac{1-\cosh 2q_\parallel}{q_\parallel \sinh 2q_\parallel}\right]. \tag{38}$$

Again we emphasize that, just as the expression (33) for $C_{zz}^{(\mathrm{E})}(\mathbf{q}_\parallel, z, z')$, the expression (38) for $C_{zz}^{(\mathrm{E})}(\mathbf{q}_\parallel)$ is indeed independent of the Reynolds number when converted to dimensional units. The explicit dependence of $C_{zz}^{(\mathrm{E})}(\mathbf{q}_\parallel)$ on the wave number $q_\parallel$ means that the correlation function for the wall-normal velocity fluctuations, even in equilibrium, is spatially long ranged and, hence, affected by confinement of the fluid between the two plates. In particular, when we take the limit $q_\parallel \to 0$ in (38), we observe that the mean intensity of the equilibrium velocity fluctuations vanishes. Thus fluctuations at extremely large wavelengths are effectively suppressed by the boundaries. On the other hand, at very short wavelengths, i.e., in the "bulk" limit $q_\parallel \to \infty$, the intensity of the fluctuations becomes $\tilde{S}\,\mathrm{Re}$, independent of the wave number and not affected by the presence of boundaries.

The spatial spectrum $C_{zz}^{(\mathrm{NE})}(\mathbf{q}_\parallel)$ of the nonequilibrium wall-normal velocity fluctuations is obtained by substituting (30) into (37). It is not possible to obtain a closed-form analytic expression for this quantity. The most compact expression we can present is:

$$\begin{aligned}\frac{C_{zz}^{(\mathrm{NE})}}{\tilde{S}\,\mathrm{Re}} &= -\frac{q_\parallel^2}{2}\sum_{N,M=0}^{\infty} \frac{q_x\,\mathrm{Re}^2\,\Xi_{NM}^{(\mathrm{NE})} X_N^* X_M}{B_N^* B_M[\Gamma_N^* + \Gamma_M]} \\ &= -\frac{1}{4}\sum_{N,M=0}^{\infty} \frac{(q_x\,\mathrm{Re})^3\,\Xi_{NM}^{(\mathrm{NE})} X_N^* X_M}{\hat{B}_N^* \hat{B}_M[1 + \frac{q_x\,\mathrm{Re}}{2q_\parallel^2}(a_N^* + a_M)]},\end{aligned} \tag{39}$$

where we have made use of the relation (36) between the actual decay rates Γ_N and the coefficient a_N and a similar relation between Γ_M^* and the coefficients a_M^*. As a consequence of the Squire symmetry transformation (discussed in the Appendix), the spatial spectrum $C_{zz}^{(\mathrm{NE})}(\mathbf{q}_\parallel)$ of the nonequilibrium fluctuations only depends on two variables, namely on the magnitude $q_\parallel$ of the wave vector $\mathbf{q}_\parallel$ and on the effective Reynolds number $\overline{\mathrm{Re}} = \mathrm{Re}\cos\varphi$.

Introducing the numerical solutions for a_N and a_M^* into (39) we can calculate $C_{zz}^{(\mathrm{NE})}(\mathbf{q}_\parallel)$. Although not completely evident from (39), the spectrum $C_{zz}^{(\mathrm{NE})}(\mathbf{q}_\parallel)$, when expressed in physical units, is roughly proportional to the square of the effective Reynolds number. This is more clearly shown in the asymptotic expansions for large and small $q_\parallel$, which are both indeed proportional to $\overline{\mathrm{Re}}^2$ exactly. For this reason we have displayed in Fig. 4 plots of the normalized spectrum $C_{zz}^{(\mathrm{NE})}(\mathbf{q}_\parallel)/\overline{\mathrm{Re}}^2$ as a function of $q_\parallel$ for three values of the effective Reynolds number $\overline{\mathrm{Re}}$ (replacing the dimensional prefactor $\tilde{S}\,\mathrm{Re}$ by unity). For two of these values, namely $\overline{\mathrm{Re}} = 25$ and $\overline{\mathrm{Re}} = 100$, the corresponding values of $a_N(q_\parallel)$ were presented

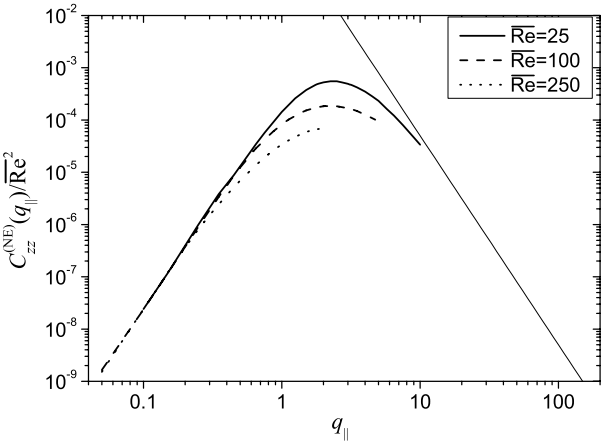

Fig. 4 Normalized nonequilibrium autocorrelation function $C_{zz}^{(\mathrm{NE})}(\mathbf{q}_\parallel)/\overline{\mathrm{Re}}^2$ of the wall-normal velocity fluctuations as a function of $q_\parallel$ for three different values of $\overline{\mathrm{Re}} = \mathrm{Re}\cos\varphi$ as indicated. The curves have been obtained by numerical evaluation of (39). The exact asymptotic $1/2q^4$ behavior for large $q_\parallel$ (common for all Reynolds numbers) is plotted, for reference, as a *thin line*

in Figs. 2 and 3. The third effective Reynolds number value displayed in Fig. 4 is $\overline{\mathrm{Re}} = 250$, which is closer to the value where the instability may manifest itself [17]. For Reynolds number substantially larger, the system is unstable and the Orr-Sommerfeld equation fails to describe the spatiotemporal evolution of the fluctuations.

In numerically computing the values displayed in Fig. 4 we truncated the double series (39) at $N = M = 11$, or less. Because of the finite number of modes, we have encountered numerical convergence problems at large wave numbers due to the rapidly oscillatory nature of the Airy functions, a problem that became increasingly serious the higher the value of the Reynolds number. In this case alternative methods to approximate the eigenvalues seem advantageous [30]. On the other hand, for large $q_\parallel$, where fluctuations become independent of the boundary conditions, explicit analytic expressions for the spectrum $C_{zz}^{(\mathrm{NE})}(\mathbf{q}_\parallel)$ of nonequilibrium fluctuations can be obtained. Specifically, in the asymptotic limit $q_\parallel \to \infty$, $C_{zz}^{(\mathrm{NE})}(\mathbf{q}_\parallel)$ becomes proportional to $q_\parallel^{-4}$ [13, 14]; this asymptotic limit is displayed in Fig. 4 as a thin line. Thus for $\overline{\mathrm{Re}} = 25$ we were indeed able to evaluate $C_{zz}^{(\mathrm{NE})}(\mathbf{q}_\parallel)$ from (39) (retaining only a limited number of modes) for sufficiently large values of $q_\parallel$ to reach the asymptotic limiting behavior proportional to $q_\parallel^{-4}$ as shown in Fig. 4. However, for larger $\overline{\mathrm{Re}}$, where the landscape of decay rates becomes progressively more complicated with the multiple crossovers described in Sect. 4.1, it became more and more difficult to include higher values of $q_\parallel$. What is evident from Fig. 4 is that, due to the boundary conditions, $C_{zz}^{(\mathrm{NE})}(\mathbf{q}_\parallel)$ goes to zero proportional to $q_\parallel^4$ in the limit $q_\parallel \to 0$.

4.3 Comparison with a Galerkin Approximation

In a previous publication [14] we evaluated the autocorrelation function for the wall-normal velocity fluctuations in a second-order Galerkin approximation. We want to compare these earlier results with the more exact results obtained here from an expansion in terms of the eigenfunctions of the Orr-Sommerfeld hydrodynamic operator.

For the equilibrium contribution to the autocorrelation function we found in the Galerkin approximation:

$$C_{zz}^{(\mathrm{E})}(q_\parallel) = \frac{7}{10}\frac{q_\parallel^2}{q_\parallel^2 + 3}\tilde{S}\,\mathrm{Re} \tag{40}$$

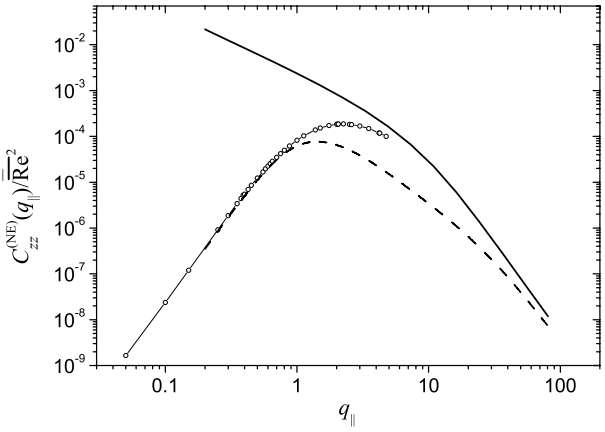

Fig. 5 Intensity of the nonequilibrium wall-normal fluctuations obtained in the present paper (*circles*) and the intensity previously obtained [14] in a Galerkin approximation (*dashed curve*) for $\overline{\mathrm{Re}} = 100$. The *solid curve* represents the exact asymptotic behavior for large $q_\parallel$ if one neglects boundary effects

to be compared with the exact result given by (38). We observe first an overall shift due to the factor 7/10 in the Galerkin approximation (40), which should be unity. In addition, the exact expression reaches the asymptotic limit $C_{zz}^{(\mathrm{E})} \simeq 1$ for large $q_\parallel \to \infty$ more slowly. Indeed, the exact expression (38) reaches this limit as $q_\parallel^{-1}$, while the Galerkin approximation (40) reaches the large $q_\parallel$ limit as $q_\parallel^{-2}$. This qualitative difference is a clear shortcoming of the Galerkin approximation.

With regards to the nonequilibrium contribution to the intensity of the wall-normal velocity fluctuations, we should note that in the previous publication [14] a distinction was made between an (absolute) intensity $C_{zz}^{(\mathrm{NE})}(\mathbf{q}_\parallel)$ and a (relative) nonequilibrium enhancement $\tilde{C}_{zz}^{(\mathrm{NE})}(\mathbf{q}_\parallel)$, such that

$$C_{zz}^{(\mathrm{NE})}(\mathbf{q}_\parallel) = C_{zz}^{(\mathrm{E})}(\mathbf{q}_\parallel)\tilde{C}_{zz}^{(\mathrm{NE})}(\mathbf{q}_\parallel). \tag{41}$$

Specifically, Fig. 1 in the previous paper [14] shows plots of the relative enhancement $\tilde{C}_{zz}^{(\mathrm{NE})}(\mathbf{q}_\parallel)$ as a function of $q_\parallel$ and not of the absolute intensity $C_{zz}^{(\mathrm{NE})}(\mathbf{q}_\parallel)$, as was mistakenly indicated by the label along the vertical axis in that figure.

To compare the results obtained in this paper with the Galerkin approximation presented in the previous publication [14], we have plotted in Fig. 5 the normalized intensity $C_{zz}^{(\mathrm{NE})}(\mathbf{q}_\parallel)/\overline{\mathrm{Re}}^2$ as a function of $q_\parallel$ for $\overline{\mathrm{Re}} = 100$. Again, as in Fig. 4, we have set the dimensional prefactor $\tilde{S}\,\mathrm{Re}$ to be equal to unity. The plot with circles represents the numerical results obtained from the expansion method in the present paper up to the maximum value of $q_\parallel$ for which the calculation was feasible for this value of the Reynolds number. The solid curve in Fig. 5 represents the exact solution which has been obtained in the absence of any boundary conditions [12–14]. This exact solution not only incorporates the asymptotic behavior for large $q_\parallel$ proportional to $q_\parallel^{-4}$, but also a crossover to a wave-number dependence proportional to $q_\parallel^{-4/3}$, first noticed by Lutsko and Dufty [12] and recovered by Wada and Sasa [13]. The dashed curve in Fig. 5 represents the Galerkin approximation for $C_{zz}^{(\mathrm{NE})}(\mathbf{q}_\parallel)/\overline{\mathrm{Re}}^2$ obtained in our previous publication [14].

Since at small $q_\parallel$, $C_{zz}^{(\mathrm{NE})}(\mathbf{q}_\parallel)$ varies as $q_\parallel^4$ and $C_{zz}^{(\mathrm{E})}(\mathbf{q}_\parallel)$ as $q_\parallel^2$, it follows from (41) that the relative nonequilibrium enhancement $\tilde{C}_{zz}^{(\mathrm{NE})}(\mathbf{q}_\parallel)$ will vanish proportional to $q_\parallel^2$ as $q_\parallel \to 0$. On the other hand, we know from the exact solution for large $q_\parallel$ that both $C_{zz}^{(\mathrm{NE})}(\mathbf{q}_\parallel)$ and $\tilde{C}_{zz}^{(\mathrm{NE})}(\mathbf{q}_\parallel)$ will vary as $q_\parallel^{-4}$ (since $C_{zz}^{(\mathrm{E})}(\mathbf{q}_\parallel)$ becomes independent of the wave number in the

bulk limit). Hence, we confirm our previous observation that the relative nonequilibrium enhancement $\tilde{C}_{zz}^{(\mathrm{NE})}(\mathbf{q}_\parallel)$ exhibits a crossover from a $q_\parallel^{-4}$ behavior for large $q_\parallel$ to a $q_\parallel^2$ behavior for small $q_\parallel$ [16].

We see in Fig. 5 that our numerical results do approach the known asymptotic behavior for large $q_\parallel$. However, we are unable to resolve the question whether a confluent singular behavior proportional to $q_\parallel^{-4/3}$ in the absence of boundary conditions [12] does or does not survive in the presence of boundary conditions. Figure 5 shows that the exact result for small values of $q_\parallel$ is in very good agreement with the estimates obtained from the Galerkin approximation. Moreover, in our previous publication we have shown that the Galerkin approximation is also in satisfactory agreement with the limiting behavior for large $q_\parallel$. However, we see from Fig. 5 that for intermediate values of $q_\parallel$ our previous Galerkin approximation underestimates the intensity of the wall-normal velocity fluctuations by a factor that can be as large as 100.

4.4 Energy Amplification Due to Thermal Noise

A quantity of considerable interest is the energy amplification associated with the velocity fluctuations. Bamieh and Dahleh [6] and Jovanovic and Bamieh [7] have investigated the energy amplification in channel flows as a result of applying stochastic forcing of nonthermal origin to the linearized Navier-Stokes equation. Our method enables us to determine the energy amplification from intrinsic thermal noise. As discussed elsewhere [14], the kinetic-energy content can be defined in terms of the "average" fluctuation in a given volume V:

$$\overline{\delta\mathbf{v}}(t) = \frac{1}{V}\int_V \delta\mathbf{v}(\mathbf{r},t)\,d\mathbf{r}. \tag{42}$$

Then the kinetic energy ε associated with the fluctuations can be obtained as:

$$\varepsilon = \tfrac{1}{2}\big\langle[\overline{\delta\mathbf{v}}(t)]^2\big\rangle = \frac{1}{2V^2}\int\!\!\int_{V\times V}\big\langle\delta v_i(\mathbf{r},t)\delta v_i(\mathbf{r}',t)\big\rangle\,d\mathbf{r}\,d\mathbf{r}', \tag{43}$$

where summation over repeated indices is understood. In stationary flow the specific energy ε does not depend on the time t. In a compressible fluid in equilibrium $M\varepsilon = (3/2)k_\mathrm{B}T$, where M is the mass contained in the volume V. If the system is incompressible, as assumed in the present paper, the equilibrium kinetic energy $M\varepsilon = k_\mathrm{B}T$, because incompressibility does not allow for independent fluctuations of the three spatial component of the velocity [27, 28]. Here we only consider the contribution to the energy amplification obtained by identifying the velocity component v_i in (43) with v_z. Considering a volume element that extends over the full height of the fluid layer, we can obtain the spatial spectrum $\varepsilon_{zz}(\mathbf{q}_\parallel)$ of the wall-normal kinetic-energy amplification from the relationship:

$$\frac{1}{8}\int_{-1}^{1}dz\int_{-1}^{1}dz'\big\langle\delta v_z^*(\mathbf{q}_\parallel,z,t)\cdot\delta v_z(\mathbf{q}_\parallel',z',t)\big\rangle = \varepsilon_{zz}(\mathbf{q}_\parallel)(2\pi)^2\delta(\mathbf{q}_\parallel-\mathbf{q}_\parallel'). \tag{44}$$

Hence, the spatial spectrum of the kinetic energy resulting from the wall-normal velocity fluctuations is simply proportional to the autocorrelation function $C_{zz}(\mathbf{q}_\parallel)$ that was discussed in Sects. 4.2–4.3. From Figs. 4 and 5 we see that C_{zz} and, hence, ε_{zz} exhibit a nonequilibrium enhancement in the presence of flow approximately proportional to the square of the Reynolds number. However, in spite of the wild behavior of the decay rates with crossover regions and crossings as described in Sect. 4.1, ε_{zz} is a smooth function of $q_\parallel$ and does remain finite at any value of the Reynolds number in agreement with the conclusions reached by other authors on the basis of stochastic forcing.

5 Discussion

We have shown how intrinsic velocity fluctuations in laminar fluid flow, that are always present in the absent of any external perturbation, can be evaluated on the basis of the method of fluctuating hydrodynamics. This method shows that wall-normal velocity fluctuations in plane Couette flow, within a linear approximation, should satisfy a stochastic Orr-Sommerfeld equation. In the absence of boundary conditions this stochastic Orr-Sommerfeld equation can be readily solved explicitly as discussed in previous works [12–14]. However, since the velocity fluctuations turn out to be spatially long ranged, the presence of boundaries cannot be neglected and it is necessary to solve the stochastic Orr-Sommerfeld equation subject to appropriate boundary conditions. In a previous publication [14] an attempt was made to solve the stochastic Orr-Sommerfeld equation in the presence of boundaries by adopting a second-order Galerkin approximation. In the present paper we have checked the Galerkin approximation by comparing it with the exact solution expressed as an expansion in terms of the eigenfunctions of the Orr-Sommerfeld hydrodynamic operator.

The flow causes an enhancement of the wall-normal velocity fluctuations. We have confirmed our previous observation, based on semi-quantitative Galerkin approximations, that the relative enhancement of the wall-normal velocity fluctuations with wave vector $\mathbf{q}_\parallel$ in the horizontal plane exhibits a crossover from a $q_\parallel^{-4}$ behavior for large $q_\parallel$ independently of boundary effects to a $q_\parallel^2$ behavior for small $q_\parallel$ as a result of the confinement of the fluid layer between two plates. The previous Galerkin approximation [14] yields good agreement with the exact limiting behavior for large and small $q_\parallel$, but underestimates somewhat the enhancement at intermediate values of the wave number. The main conclusion of this investigation is that the flow-induced enhancement of the velocity fluctuations increases with the Reynolds number approximately as Re^2. The actual amplitude strongly depends on the wave number, as shown in Fig. 4. The enhancement of spontaneous thermal fluctuations is considered nowadays a generic feature [3, 29] of systems outside of equilibrium, arising from mode-coupling effects that are not present in equilibrium. The nonequilibrium enhancement described in this paper is due to the coupling between δv_z modes with different horizontal wave vectors that is implicit in the second term of the Orr-Sommerfeld equation (1).

Previous studies of energy amplification of disturbances in shear flows have shown that the dominant contribution arises from a coupling of the Orr-Sommerfeld and Squire equations [4–7]. Our previous investigation, based on a Galerkin approximation, has indicated that the same feature holds for the nonequilibrium amplification of the thermal noise [14, 15]. Therefore, the next important question is how the exact solution of the stochastic Orr-Sommerfeld equation obtained in the present paper, will couple with the stochastic Squire equation. We plan to address this issue in a subsequent publication.

Acknowledgements J.V.S. acknowledges the hospitality of the Departamento de Física Aplicada I, Universidad Complutense de Madrid, where part of the article was prepared. The research was supported by the Spanish Ministry of Science and Innovation through research grant FIS2008-03801.

Appendix: Analytical Expression of the Hydrodynamic Modes and Their Corresponding Decay Rates

With the definition:

$$\left(\partial_z^2 - q_\parallel^2\right) R_N(\mathbf{q}_\parallel, z) = P_N(\mathbf{q}_\parallel, z), \tag{45}$$

we can rewrite (10) for the right hydrodynamic modes, with $\mathcal{H}$ given by (7), as an equation for $P_N(\mathbf{q}_\parallel, z)$ whose general solution can be expressed as a combination of Airy functions [31], namely:

$$P_N(\mathbf{q}_\parallel, z) = A_0 \operatorname{Ai}\big[(q_x \operatorname{Re})^{1/3}(a_N - \mathrm{i}z)\big] - A_1 \operatorname{Bi}\big[(q_x \operatorname{Re})^{1/3}(a_N - \mathrm{i}z)\big], \tag{46}$$

where A_0 and A_1 are two integration constants to be determined later, while the parameter a_N depends on the wave vector $\mathbf{q}_\parallel$ of the fluctuations and is related to the decay rate $\Gamma_N(\mathbf{q}_\parallel)$ by:

$$\Gamma_N(\mathbf{q}_\parallel) = q_x a_N(\mathbf{q}_\parallel) + \frac{q_\parallel^2}{\operatorname{Re}}. \tag{47}$$

The right eigenfunctions R_N can be obtained by integrating (45) and imposing the boundary conditions (11). Some straightforward analysis shows that the right eigenfunctions can be simply expressed by:

$$R_N(\mathbf{q}_\parallel, z) = \frac{1}{q_\parallel} \int_{-1}^{z} P_N(\mathbf{q}_\parallel, \xi) \sinh(q_\parallel(z - \xi))\, d\xi, \tag{48}$$

where $P_N(\mathbf{q}_\parallel, z)$, given by (46), has to satisfy the following two conditions:

$$\begin{aligned} \int_{-1}^{1} P_N(t) \sinh(q_\parallel(t-1))\, dt &= 0, \\ \int_{-1}^{1} P_N(t) \cosh(q_\parallel(t-1))\, dt &= 0. \end{aligned} \tag{49}$$

The first of the conditions (49) can be readily satisfied for given values of $\mathbf{q}_\parallel$ and Re (and, thus, for any a_N) by choosing the integration constants A_0 and A_1 in (46) such that:

$$\begin{aligned} A_0 &= \int_{-1}^{1} \operatorname{Bi}\big[(q_x \operatorname{Re})^{1/3}(a_N - \mathrm{i}t)\big] \sinh(q_\parallel(t-1))\, dt, \\ A_1 &= \int_{-1}^{1} \operatorname{Ai}\big[(q_x \operatorname{Re})^{1/3}(a_N - \mathrm{i}t)\big] \sinh(q_\parallel(t-1))\, dt. \end{aligned} \tag{50}$$

However, satisfying the second of the conditions (49) is not so trivial. Upon substitution of (50) into (46), the second of (48) becomes:

$$\begin{aligned} &\int_{-1}^{1} A(t) \sinh(q_\parallel t)\, dt \int_{-1}^{1} B(t) \cosh(q_\parallel t)\, dt \\ &\quad = \int_{-1}^{1} A(t) \cosh(q_\parallel t)\, dt \int_{-1}^{1} B(t) \sinh(q_\parallel t)\, dt, \end{aligned} \tag{51}$$

where, to simplify the notation, we have adopted the following abbreviations:

$$\begin{aligned} A(z) &= \operatorname{Ai}\big[(q_x \operatorname{Re})^{1/3}(a_N - \mathrm{i}z)\big], \\ B(z) &= \operatorname{Bi}\big[(q_x \operatorname{Re})^{1/3}(a_N - \mathrm{i}z)\big]. \end{aligned} \tag{52}$$

We consider condition (51), for given values of $\mathbf{q}_\parallel$ and Re, as an equation to obtain a_N and, then the decay rate $\Gamma_N(\mathbf{q}_\parallel)$, through (47). In general, the solutions of (51) for a_N

can only be obtained numerically, and some numerical results are presented in Sect. 4.1. Due to the oscillatory character of the Airy functions, there exists an infinite numerable set of solutions. By introducing a modified Reynolds number as $\overline{\mathrm{Re}} = \mathrm{Re}\cos\varphi$ (with φ the azimuthal angle, so that $q_x = q_\parallel \cos\varphi$), we note that the solution of (51) for a_N depends only on the magnitude $q_\parallel$ of the horizontal wave number and on the modified Reynolds number $\overline{\mathrm{Re}}$. This symmetry of the decay rates is well known, and usually referred to as the Squire transformation [18]. As shown elsewhere [6, 7, 32], for the particular case of streamwise modes ($q_x = 0$) (48) and (51) simplify appreciably, and it then becomes possible to obtain more explicit expressions (not involving integrations) for the normal-modes and for the decay rates.

In the general case, the left eigenfunction corresponding to an eigenvalue a_N solution of (51) can also be expressed analytically in terms of integrals of Airy functions. The solution of (13) is

$$L_N(z) = \frac{\mathrm{i}\pi\,\mathrm{Re}}{(q_x\,\mathrm{Re})^{1/3}} \int_{-1}^{z} \big[A^*(z)B^*(t) - A^*(t)B^*(z)\big]\big[B_0\cosh(q_\parallel t) - B_1\sinh(q_\parallel t)\big]\,dt. \quad (53)$$

We observe that the solution (53) vanishes and has a zero vertical derivative at $z = -1$, independent of the integration constants B_0 and B_1. Imposing the boundary conditions at $z = 1$, we conclude after some analysis that the left mode $L_N(z)$ and its z-derivative will be zero at $z = 1$, if and only if the two following conditions are met:

$$\begin{aligned} \int_{-1}^{1} A^*(t)\big[B_0\cosh(q_\parallel t) - B_1\sinh(q_\parallel t)\big]\,dt = 0, \\ \int_{-1}^{1} B^*(t)\big[B_0\cosh(q_\parallel t) - B_1\sinh(q_\parallel t)\big]\,dt = 0. \end{aligned} \quad (54)$$

The first of the conditions (54) can be readily satisfied for any given values of $\mathbf{q}_\parallel$ and Re. For instance, one can just choose the integration constants B_0 and B_1 such that:

$$B_0 = \int_{-1}^{1} A^*(t)\sinh(q_\parallel t)\,dt, \qquad B_1 = \int_{-1}^{1} A^*(t)\cosh(q_\parallel t)\,dt. \quad (55)$$

However, to satisfy the second of the conditions (54) and to obtain a valid nonzero $L_N(z)$, we need to consider a more complicated expression, that is similar to (51) except that the arguments of the Airy functions now appear as complex conjugates. Since the Airy functions have the property $\mathrm{Ai}(z^*) = \mathrm{Ai}^*(z)$ (and the same for Bi), if a_N is a solution of (51), then a_N^* will be a solution of a similar equation obtained by replacing $(a_N - \mathrm{i}t)$ by $(a_N^* + \mathrm{i}t)$ in the argument of the Airy functions. Hence, the left eigenvalues are the complex conjugate of the right eigenvalues.

So far, we have considered the left and right hydrodynamic modes with arbitrary normalization. For a complete specification of the modes we must evaluate the normalization constants $B_N(\mathbf{q}_\parallel)$, as defined by (14). First of all, we observe that the expression for $B_N(\mathbf{q}_\parallel)$ can be simplified with the help of (45), so that:

$$B_N(\mathbf{q}_\parallel) = \int_{-1}^{1} L_N^*(\mathbf{q}_\parallel, t)\,P_N(\mathbf{q}_\parallel, t)\,dt. \quad (56)$$

Substituting (46) and (53) into (56), we find that the resulting integral can be evaluated analytically after integrating by parts and using the Wronskian of the Airy functions [31]

with the result:

$$B_N(\mathbf{q}_\parallel) = -\frac{\mathrm{i}}{q_x}\hat{B}_N(\overline{\mathrm{Re}}, q_\parallel) \tag{57}$$

with

$$\begin{aligned}\hat{B}_N(\overline{\mathrm{Re}}, q_\parallel) = {} & P_N(\mathbf{q}_\parallel, 1)\big[B_0^* \cosh(q_\parallel) - B_1^* \sinh(q_\parallel)\big] \\ & - P_N(\mathbf{q}_\parallel, -1)\big[B_0^* \cosh(q_\parallel) + B_1^* \sinh(q_\parallel)\big].\end{aligned} \tag{58}$$

Again, because of the Squire symmetry, the coefficients $\hat{B}_N$ depend only on the magnitude $q_\parallel$ and the product $q_x\,\mathrm{Re}$ (or on wave number $q_\parallel$ and modified Reynolds number $\overline{\mathrm{Re}}$).

Another quantity required to discuss the energy amplification is the vertical integration of the right modes, X_N:

$$X_N(\overline{\mathrm{Re}}, q_\parallel) = \int_{-1}^{1} R_N(\mathbf{q}_\parallel, t)\,dt = -\frac{1}{q_\parallel^2}\int_{-1}^{1} P_N(\mathbf{q}_\parallel, t)\,dt. \tag{59}$$

The integral (59) can be expressed analytically in terms of Scorer functions [31], but the corresponding expression is quite long and not very informative. We do not display it here, but we have used this analytic expression in the numerical computations. Again, due to the Squire symmetry, X_N depends only on the magnitude $q_\parallel$ and on the product $q_x\,\mathrm{Re}$. To complete the discussion of the Squire symmetry, we note that due to the multiplicative prefactor Re in the expression (53) for the left eigenfunctions, the nonequilibrium mode-coupling coefficients $\Xi_{NM}^{(\mathrm{NE})}(\mathbf{q}_\parallel)$, as defined by (23), will also depend only on the magnitude $q_\parallel$ and on the product $q_x\,\mathrm{Re}$.

References

1. Landau, L.D., Lifshitz, E.M.: Fluid Mechanics, 2nd edn. Pergamon, Oxford (1987)
2. Fox, R.F., Uhlenbeck, G.E.: Contributions to non-equilibrium thermodynamics. I. Theory of hydrodynamical fluctuations. Phys. Fluids **13**, 1893–1902 (1970)
3. Ortiz de Zárate, J.M., Sengers, J.V.: Hydrodynamic Fluctuations in Fluids and Fluid Mixtures. Elsevier, Amsterdam (2006)
4. Farrell, B.F., Ioannou, P.J.: Stochastic forcing of the linearized Navier-Stokes equations. Phys. Fluids A, Fluid Dyn. **5**, 2600–2609 (1993)
5. Farrell, B.F., Ioannou, P.J.: Variance maintained by stochastic forcing of non-normal dynamical systems associated with linearly stable shear flows. Phys. Rev. Lett. **72**, 1188–1191 (1994)
6. Bamieh, B., Dahleh, M.: Energy amplification in channel flows with stochastic excitation. Phys. Fluids **13**, 3258–3269 (2001)
7. Jovanovic, M.R., Bamieh, B.: Componentwise energy amplification in channel flows. J. Fluid Mech. **534**, 145–183 (2005)
8. Eckhardt, B., Pandit, R.: Noise correlations in shear flows. Eur. Phys. J. B **33**, 373–378 (2003)
9. Tremblay, A.-M.S., Arai, M., Siggia, E.D.: Fluctuations about simple nonequilibrium states. Phys. Rev. A **23**, 1451–1480 (1981)
10. Dufty, J.W., Lutsko, J.: Structure and stability of hydrodynamic models for shear flow. KINAM **6**, 169–181 (1984)
11. Lutsko, J.F., Dufty, J.W.: Hydrodynamic fluctuations at large shear rate. Phys. Rev. A **32**, 3040–3054 (1985)
12. Lutsko, J.F., Dufty, J.W.: Long-ranged correlations in sheared fluids. Phys. Rev. E **66**, 041206 (2002)
13. Wada, H., Sasa, S.-I.: Anomalous pressure in fluctuating shear flow. Phys. Rev. E **67**, 065302R (2003)
14. Ortiz de Zárate, J.M., Sengers, J.V.: Transverse-velocity fluctuations in a liquid under steady shear. Phys. Rev. E **77**, 026306 (2008)

15. Ortiz de Zárate, J.M., Sengers, J.V.: Nonequilibrium velocity fluctuations and energy amplification in planar Couette flow. Phys. Rev. E **79**, 046308 (2009)
16. Sengers, J.V., Ortiz de Zárate, J.M.: Velocity fluctuations in laminar fluid flow. J. Non-Newton. Fluid Mech. **165**, 925–931 (2010)
17. Schmid, P.J., Henningson, D.S.: Stability and Transition in Shear Flows. Springer, Berlin (2001)
18. Drazin, P.G., Reid, W.H.: Hydrodynamic Stability, 2nd edn. Cambridge University Press, Cambridge (2004)
19. Grossmann, S.: The onset of shear flow turbulence. Rev. Mod. Phys. **72**, 603–618 (2000)
20. Sagués, F., Sancho, J.M., García-Ojalvo, J.: Spatiotemporal order out of noise. Rev. Mod. Phys. **79**, 829–882 (2007)
21. Mannevile, P.: Instabilities, Chaos, and Turbulence, 2nd edn. World Scientific, Singapore (2010)
22. Schmitz, R., Cohen, E.G.D.: Fluctuations in a fluid under a stationary heat flux. I. General theory. J. Stat. Phys. **39**, 285–316 (1985)
23. Schmitz, R., Cohen, E.G.D.: Fluctuations in a fluid under a stationary heat flux. II. Slow part of the correlation matrix. J. Stat. Phys. **40**, 431–316 (1985)
24. Zubarev, D.N., Morozov, V.G.: Statistical mechanics of nonlinear hydrodynamic fluctuations. Physica A **120**, 411–467 (1983)
25. Romanov, V.A.: Stability of the plane Couette flow. Dokl. Akad. Nauk SSSR **196**, 1049–1051 (1971)
26. Dyachenko, A.V., Shkalikov, A.A.: On a model problem for the Orr-Sommerfeld equation with linear profile. Funct. Anal. Appl. **36**, 228–232 (2002)
27. Boon, J.P., Yip, S.: Molecular Hydrodynamics. McGraw-Hill, New York (1980), Dover edition (1991)
28. Hansen, J.P., McDonald, I.R.: Theory of Simple Liquids, 2nd edn. Academic Press, London (1986)
29. Kirkpatrick, T.R., Belitz, D., Sengers, J.V.: Long-time tails, weak localization, and classical and quantum critical behavior. J. Stat. Phys. **109**, 373–405 (2002)
30. Skorokhodov, S.L.: Numerical analysis of the spectrum of the Orr-Sommerfeld problem. Comput. Math. Math. Phys. **47**, 1603–1621 (2007)
31. Abramowitz, M., Stegun, I.A.: Handbook of Mathematical Functions. Dover, New York (1964)
32. Dolph, C.L., Lewis, D.C.: On the application of infinite systems of ordinary differential equations to perturbations of plane Poiseuille flow. Q. Appl. Math. **16**, 97–110 (1958)